# Radicals Produced by $\gamma$-Irradiation of Hyperquenched Glassy Water Containing 2′-Deoxyguanosine-5′-monophosphate

**Justyna Staluszka,[†] Malgorzata Steblecka,[†] Ewa Szajdzinska-Pietek,*[,†] Ingrid Kohl,[‡] Christoph G. Salzmann,[‡] Andreas Hallbrucker,[‡] and Erwin Mayer[‡]**

*Institute of Applied Radiation Chemistry, Technical University of Lodz, Wroblewskiego 15, 93-590 Lodz, Poland, and Institute of General, Inorganic and Theoretical Chemistry, Innsbruck University, A-6020 Innsbruck, Austria*

*Received: April 29, 2008; Revised Manuscript Received: June 30, 2008*

Hyperquenched glassy water (HGW) has been suggested as the best model for liquid water, to be used in low-temperature studies of indirect radiation effects on dissolved biomolecules (Bednarek et al. *J. Am. Chem. Soc.* **1996**, *118*, 9387). In the present work, these effects are examined by X-band electron spin resonance spectroscopy (ESR) in $\gamma$-irradiated HGW matrix containing 2′-deoxyguanosine-5′-monophosphate. Analysis of the complex ESR spectra indicates that, in addition to $OH^{\cdot}$ and $HO_2^{\cdot}$ radicals generated by water radiolysis, three species are trapped at 77 K: (i) $G(C8)H^{\cdot}$ radical, the H-adduct to the double bond at C8; (ii) $G^{-\cdot}$ radical anion, the product of electron scavenging by the aromatic ring of the base; and (iii) $dR(-H)^{\cdot}$ radicals formed by H abstraction from the sugar moiety, predominantly at the C′5 position. We discuss the yields of the radicals, their thermal stability and transformations, as well as the effect of photobleaching. This study confirms our earlier suggestion that in HGW the H atom addition/abstraction products are created at 77 K in competition with $HO_2^{\cdot}$ radicals, in a concerted process following ionization of water molecule at L-type defect sites of the H-bonded matrix. The lack of $OH^{\cdot}$ reactivity toward the solute suggests that the H-bonded structure in HGW is much more effective in recombining $OH^{\cdot}$ radicals than that of aqueous glasses obtained from highly concentrated electrolyte solutions. Furthermore, complementary experiments for the neat matrix have provided evidence that $HO_2^{\cdot}$ radicals are not the product of H atom reaction with molecular oxygen, possibly generated by ultrasounds used in the process of sample preparation.

## Introduction

Radicals generated by high-energy irradiation of liquid water are one of the primary sources of radiation damage to biomolecules.[1] These radicals are short-lived at ambient temperature, and therefore low-temperature electron spin resonance spectroscopy (ESR) is a method of choice to follow their reactions and resulting paramagnetic products.[2,3] In studies of radiation damage to DNA, aqueous solutions of nucleobases, nucleosides, and nucleotides are widely used as model systems. However, on cooling dilute aqueous solutions in liquid nitrogen, phase-separated systems are obtained, and solute molecules become freeze-concentrated in microdomains suspended in the aqueous matrix of ice *Ih*.[4] In such systems, the primary products of bulk water radiolysis are trapped in the ice compartments and are unable to interact with solutes;[5] thus, the direct radiation effects on the solute are mainly observed, if its concentration is high enough, cf., ref 6. The prerequisite to observe indirect radiation effects beyond the first solvation shell is a homogeneous distribution of the solute, and this occurs at low temperatures in glassy matrices, such as concentrated electrolyte solutions frozen at 77 K.

Recently, Plonka et al. introduced hyperquenched glassy water, HGW, as a new matrix for radiation cryochemical studies.[7−10] It can be obtained by cooling micrometer-sized droplets of liquid water with the rate of $10^6-10^7$ K/s.[11] An advantage in using glassy water or glassy dilute aqueous solutions made by hyperquenching over concentrated aqueous electrolyte glasses made by slow cooling is that the former systems contain bulk water, whereas in the latter systems nearly all water is involved in hydration of added ions. Besides, in HGW systems, unlike electrolyte glasses, no radicals are generated from inorganic additives, which might obscure the reactions of water radiolysis products with the substrate.

The specific feature of HGW, in comparison to ice *Ih*, is formation of hydroperoxyl radicals, in addition to hydroxyl radicals, at the primary step of radiolysis.[7] This has been attributed to the relatively high concentration of so-called L-type defect sites[12] in the hydrogen-bonded structure of HGW. It has been postulated that ionization of a water molecule at such a site is followed by a concerted process including formation of an O−O bond (leading to $HO_2$), release of a hydrogen molecule, and formation of a hydronium ion.[7,10]

In our earlier studies, the solute-derived radicals have been observed at 77 K in $\gamma$-irradiated HGW matrices containing thymine, 2′-deoxythymidyne, 2-deoxy-D-ribose, and an equimolar mixture of 2-deoxy-D-ribose and thymine, in concentration as low as 5 mmol/dm$^3$. They were identified as radical anions of the base, formed by electron scavenging, and neutral radicals formed by H-atom reactions with the solute. It was suggested that the latter reactions occur in competition with $HO_2^{\cdot}$ formation at the L-type defect sites.[9,13]

In the present work, we report the ESR study of $\gamma$-irradiated glassy solution of 2′-deoxyguanosine-5′-monophosphate (dGMP/HGW system), cf., Chart 1. Our objectives were to identify

* Corresponding author. Phone: 48-42-6313189. Fax: 48-42-6840043. E-mail: espietek@mitr.p.lodz.pl.
[†] Technical University of Lodz.
[‡] Innsbruck University.

10.1021/jp8037544 CCC: $40.75 
Published on Web 08/26/2008

**CHART 1: 2′-Deoxyguanosine-5′-monophosphate (dGMP)**

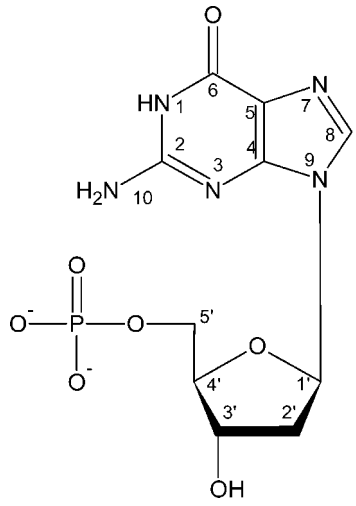

paramagnetic species trapped at 77 K, to assess their yields and thermal stability, and to compare the results with those reported for irradiated guanine derivatives in other matrices. Despite numerous low-temperature ESR studies on radiolysis of aqueous systems containing DNA and its constituents, there are still controversies on the assignment of the observed signals and mechanisms of radical formation.[2,3] An additional objective of our study was further evaluation of the usefulness of HGW as a matrix for stabilization of primary radiolysis products.

## Experimental Section

dGMP (sodium salt, 98−100%) from Sigma-Aldrich was used as received. The 50 mmol/dm$^3$ dGMP solutions were prepared in deionized water saturated with gaseous $N_2$ (99.999%). Glassy samples were obtained from aqueous droplets made by means of an ultrasonic nebulizer (HICO Ultrasonat, model 706E, operating at 1.7 MHz); details of the procedure have been described earlier.[7−11] HGW samples characterized by X-ray diffraction contained at most 5% crystalline, mainly cubic, ice, whereas HGW samples characterized by neutron scattering showed no evidence for any residual crystallinity.[14] The difference may reflect that neutrons are essentially a bulk probe whereas X-rays are sensitive to surface effects. One hour of deposition of micrometer-sized droplets produced a 2−3 mm thick opaque layer of glassy solid water with a porcelain-like appearance and texture. We note that the opaqueness is caused by stray light on the hyperquenched droplets, and the gaps and cavities in between (cf., Figure 2 in ref 15), and not by crystalline ice.

Neat HGW was also prepared with the use of a pneumatic nebulizer (a retouching air brush, Grafo type I). For the pneumatic nebulizer, droplet size and distribution is not known, but it is certainly larger than those of the ultrasonic nebulizer. Because of that, samples made with the pneumatic nebulizer contained a significant fraction of crystalline ice (up to 50%), yet they were examined to ascertain that sonification had no effect on the kind of primary radicals formed due to irradiation.

The samples were irradiated at 77 K for 160 min with a $^{60}$Co γ-source at a dose rate of 3.0 ± 0.2 kGy/h. X-band ESR spectra were recorded with a Bruker ER 200D-SRC spectrometer, on line with an ESP 3220-200SH system for data acquisition and processing, employing a 100 kHz field modulation of amplitude 5 G and different microwave powers. The $Cr^{3+}$/MgO standard was used to normalize the spectra for frequency. ESR measurements were done at 77 K, immediately after irradiation and after successive annealing of the samples (outside the ESR cavity) at temperatures in the range 120−270 K for 5 min. Primary experiments were performed in dark to avoid incidental photobleaching of irradiated samples. To assess the effect of photobleaching, the experiments were repeated with new samples exposed (after γ-irradiation) to a wide band visible light for 20 min at 77 K. A 150 W halogen lamp was used as a light source.

Quantitative determinations were done by doubly integrating the spectra acquired at the microwave power of 0.02 mW, and a frozen solution of DPPH in benzene was used as a standard to evaluate the yields of radicals at 77 K, cf., ref 16 for details.

In the following section, we will present experimental spectra acquired at the microwave power of 0.02 mW, unless indicated otherwise. Simulated spectra have been obtained using WinEPR SimFonia software from Bruker (version 1.25). Coaxial *g* and *A* tensors have been assumed, and simulations were carried out to the second order of approximation, without forbidden transitions. For reconstructing experimental spectra with the component signals, we have used a homemade program based on the least-squares optimization described by others.[17]

## Results and Discussion

**Radicals Produced in Neat HGW.** The present results for irradiated HGW samples prepared with the use of ultrasonic nebulizer are consistent with the previous study.[7] ESR spectra consist of two components corresponding to $OH^{\bullet}$ and $HO_2^{\bullet}$ radicals, which are formed in equal amounts. The total radical concentration determined in this work is 0.70 ± 0.04 mmol/dm$^3$ at the absorbed dose of 8 kGy, in agreement with the radiation yield reported earlier, $G = 0.83$ spins per 100 eV.[18]

It has been argued (at the Miller Conference on Radiation Chemistry, 2003) that $HO_2^{\bullet}$ radicals in HGW may be formed via the reaction of molecular oxygen, possibly generated by water sonolysis in the stage of sample preparation, with radiation-produced hydrogen atoms at 77 K. Because of that, it is important to show that similar spectra were recorded for the samples prepared with the use of a pneumatic nebulizer, cf., Figure 1. There is no doubt that $HO_2^{\bullet}$ radicals are also present in these samples; their signal remains as the only spectral component after annealing at 120 K. This result refutes the above-mentioned supposition and supports the proposed mechanism of $HO_2^{\bullet}$ formation at L-type defect sites in the primary step of radiolysis.[7] It is relevant to add that $HO_2^{\bullet}$ radicals were also observed, after low-dose irradiation, in vapor-deposited amorphous solid water (prepared without ultrasonic treatment), which like HGW is rich in L-type defect sites.[8]

As seen from Figure 1b, the significant fraction of crystalline ice in HGW made with a pneumatic nebulizer does not seem to have an effect on the $HO_2^{\bullet}$ yield. However, we previously found that HGW samples made by hyperquenching large droplets (≤25 μM diameter) contain mainly cubic ice as crystalline component (cf., ref 11 and Figure 3b therein) and that this type of γ-irradiated cubic ice has relative $OH^{\bullet}/HO_2^{\bullet}$ yields similar to those of HGW (cf., Figure 4 in ref 10). The latter finding had been rationalized by the presence of defects in cubic ice.[8,10] Thus, HGW samples containing varying amounts of cubic ice can have similar $[OH^{\bullet}]/[HO_2^{\bullet}]$ ratios.

**Multicomponent Experimental Spectra of HGW/dGMP Samples.** Figure 2 presents ESR spectra recorded at 77 K for the dGMP/HGW system immediately after irradiation, and after successive annealing of the sample at higher temperatures. The

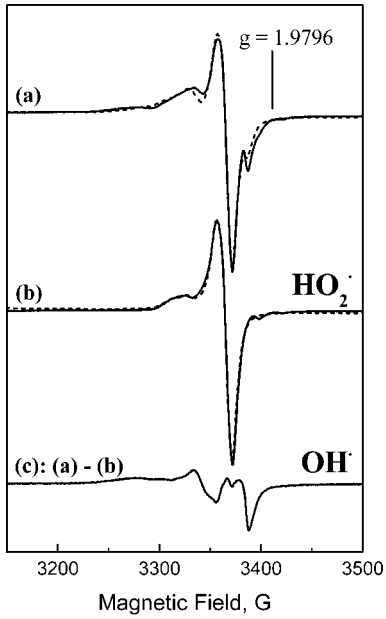


**Figure 1.** ESR spectra of $\gamma$-irradiated neat HGW samples prepared with the use of ultrasonic nebulizer (−) and pneumatic nebulizer (- - -). The spectra were recorded at 77 K using the microwave power of 2 mW, immediately after irradiation (a) and after annealing at 120 K (b); (c) is the difference spectrum for the ultrasonically nebulized sample and represents $OH^{\cdot}$ radicals in the glassy matrix.[7]

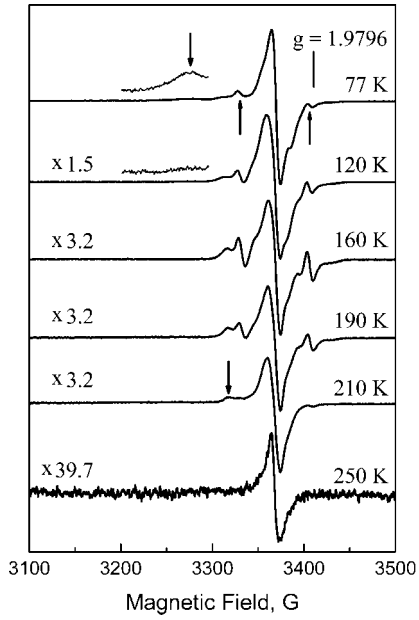


**Figure 2.** ESR spectra for the dGMP/HGW sample, recorded at 77 K immediately after $\gamma$-irradiation (77 K spectrum) and after thermal annealing at increasing temperatures (120−250 K spectra). Downward arrows indicate the $g_{||}$ line of $OH^{\cdot}$ radicals (a zoomed part of the 77 K spectrum) and that of peroxyl radicals (the 210 K spectrum); upward arrows indicate the lines of $G(C8)H^{\cdot}$ radicals; the numbers at the left-hand side denote gain increase.

initial spectrum (nonannealed sample) is distinctly different from that obtained for neat HGW, indicating the presence of solute-derived radicals in addition to $OH^{\cdot}$ and $HO_2^{\cdot}$ radicals. A zoomed part of the initial spectrum reveals the broad low-field line characteristic for $OH^{\cdot}$ radicals in glassy systems; as in neat HGW, it disappears on annealing the sample at 120 K.

The total concentration of radicals generated by 8 kGy irradiation of the dGMP/HGW system at 77 K is 1.50 ± 0.13 mmol/dm$^3$, about 2-fold higher than that in neat HGW, and about 20% decrease of the ESR intensity occurred due to 20 min of photobleaching with a wide band visible light. An obvious reason for the increased radical yield in the presence of dGMP is electron scavenging by the solute leading to formation of radical-anions and their protonated successors (electrons are not trapped in neat HGW). Another reason may be less efficient mutual electron−hole recombination resulting in an increased yield of OH radicals (cf., the data in Table 1).

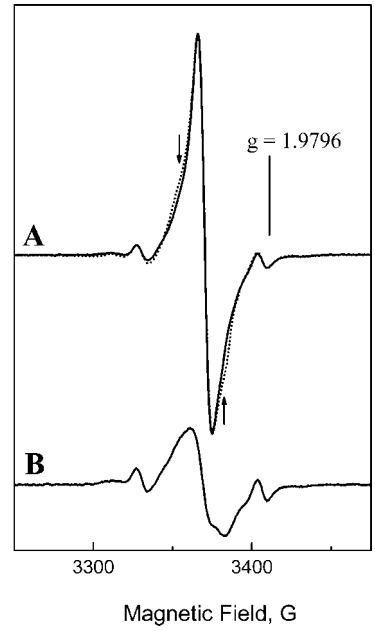


**Figure 3.** ESR signals of solute radicals trapped at 77 K in the dGMP/HGW system before (A) and after photobleaching (B). −, obtained as a difference between the spectra acquired at 40 and 20 dB; • • •, obtained by subtracting OH and $HO_2$ contribution from the initial 40 dB spectrum. See text for details.

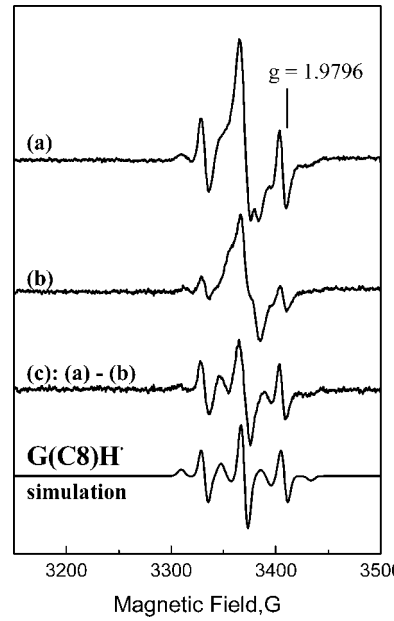


**Figure 4.** Separation of $G(C8)H^{\cdot}$ signal: (a) ESR spectrum of the dGMP/HGW sample annealed at 160 K, from which the signal of peroxyl radicals has been removed (cf., text); (b) analogous spectrum of the sample annealed at 200 K (intensity adjusted by "spectral titration" procedure); (c) difference between (a) and (b); bottom spectrum, simulated signal of $G(C8)H^{\cdot}$ radical. Simulation parameters: $a_H$ = 38 G (for 2 H atoms at C8), $A_N$ [24; 0; 0] G (for N7), $A_N'$ [4; 0; 0 G] (for N9), $g$ [2.0022; 2.0034; 2.0038], line width 6 G.[19]

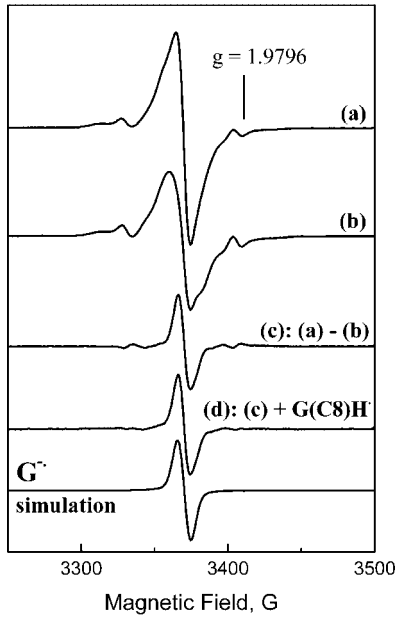


**Figure 5.** Separation of the $G^{-\cdot}$ signal: (a) initial spectrum of the dGMP/HGW sample minus contribution of OH· radicals; (b) spectrum recorded after sample annealing at 120 K; (c) difference between (a) and (b); (d) spectrum (c) corrected for a contribution of the reverse-phase G(C8)H· signal. Bottom spectrum, simulated signal of $G^{-\cdot}$ anion-radical; simulation parameters: $A_{H(C8)}$ [5.5; 3.0; 0.5] G, $g$ [2.0028; 2.0037; 2.0026], line width 6 G.[25,26]

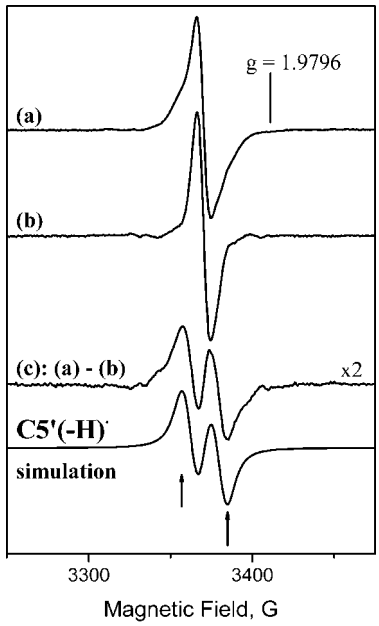


**Figure 6.** Separation of the signal of sugar radicals: (a) spectrum A of Figure 3, from which the G(C8)H· signal has been removed; (b) $G^{-\cdot}$ singlet (49% contribution to (a)); (c) difference between (a) and (b). Bottom spectrum, simulated signal of C5′(−H)· radical; simulation parameters: $A_{H(C5')}$ [7.7; 15.5; 24.5] G, $a_{H(C4')}$= 4 G, $g$ [2.0036; 2.0020; 2.0031], line width 8 G;[35,38] the distance between arrows is about 28 G.

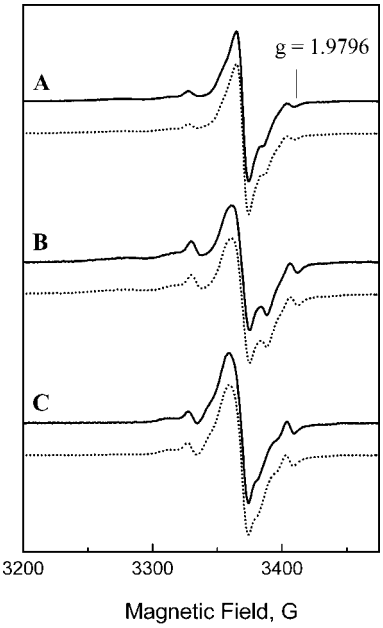


**Figure 7.** Reconstructed spectra of irradiated dGMP/HGW (• • •), as compared to experimental spectra (−): (A) initial sample, (B) photobleached sample, (C) sample annealed at 120 K. See Table 1 for the fractions of component signals relative to the total radical yield in the initial spectrum.

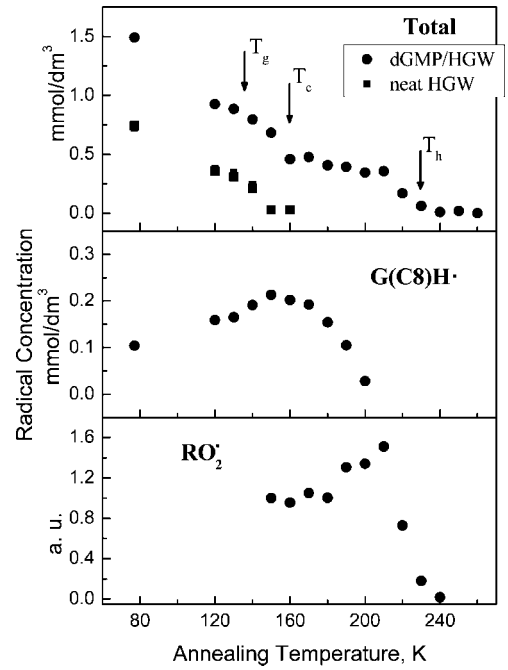


**Figure 8.** Changes of radical concentration on sample annealing: Upper panel: total radical concentration in the presence of dGMP as compared to neat HGW; arrows indicate temperatures of glass transition ($T_g$), crystallization to cubic ice ($T_c$), and transformation to hexagonal ice ($T_h$). Middle panel: G(C8)H· concentration in the dGMP/HGW sample. Lower panel: relative changes of peroxyl radical concentration in the dGMP/HGW sample.

The signals of solute-derived radicals, unlike the signals of OH· and $HO_2$· radicals, undergo significant saturation with increasing microwave power up to 2 mW. Thus, subtraction of the initial spectrum acquired at 2 mW (20 dB attenuation) from that acquired at 0.02 mW (40 dB attenuation), after normalization for the intensity of the characteristic OH· line, gives the spectrum corresponding to dGMP-derived radicals. As seen from Figure 3, this is a multicomponent spectrum, and its line shape is markedly affected by photobleaching; in particular, the intensity of the central line significantly decreases, and that of external lines increases.

The dotted line in Figure 3 represents the spectrum of solute radicals obtained by subtracting from the original low-power pattern the OH· contribution (given by the low-field line intensity), and then the $HO_2$· signal in the correct proportion determined from final analysis of our data (vide infra). It is

**TABLE 1: Relative Contributions of Radicals in the γ-Irradiated (8 kGy) HGW/dGMP (50 mmol/dm³) System, with Respect to Total Concentration Immediately after Irradiation (Initial Sample) (Uncertainty ≤10%)**

| sample | $OH^{\bullet}$ | $HO_2^{\bullet}$ | $G(C8)H^{\bullet}$ | $G^{-\bullet}$ | $dR(-H)^{\bullet}$ |
|---|---|---|---|---|---|
| initial | 0.38 | 0.22 | 0.07 | 0.17 | 0.16 |
| photobleached | 0.35 | 0.22 | 0.10 | 0.03 | 0.11 |
| annealed at 120 K | 0 | 0.25 | 0.11 | 0.08 | 0.17 |

**CHART 2: dGMP-Derived Radicals Assigned to the Observed Spectral Components**

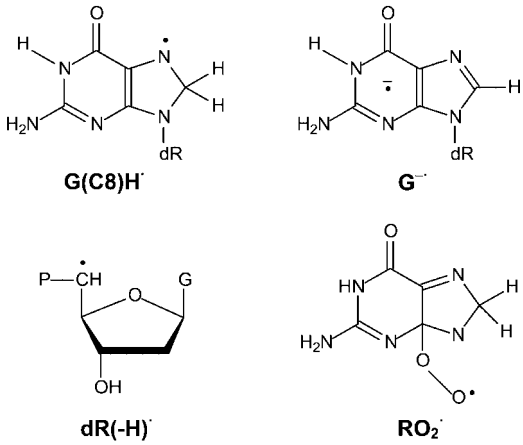


dR: 2'-deoxyribose 5'-monophosphate group

P: phosphate group

G: guanine base

somewhat different from the (40−20) dB spectrum, suggesting that the fractions of individual components are not the same in the two spectra, because of their different saturation characteristics. The shoulders indicated by arrows, separated by ∼28 G, are less intense in the difference spectrum. We will see below that this extreme line separation corresponds to sugar radicals (cf., Figure 6), which apparently are less saturable than the radicals centered at guanine.

**Identification of Solute Radicals Trapped at 77 K.** It will be shown in this section that the spectra of Figure 3 comprise three component signals; see Chart 2 for the formulas of the corresponding paramagnetic species.

**G(C8)H· Radical.** Trapping of this species at 77 K is immediately suggested by the presence of low-intensity external lines indicated by upward arrows in the spectrum of Figure 2. Their amplitudes evidently decrease on annealing the samples in the temperature range 160−200 K, and at the same time we notice the growth of the signal of peroxyl radicals (cf., Figure 8). The latter hardly saturates with increasing microwave power, so it can be removed from the spectra recorded at 0.02 mW by subtracting the respective spectra recorded at 2 mW, normalized for the intensity of the characteristic $g_{||}$ line of peroxyl radicals (cf., the 210 K spectrum in Figure 2). As shown in Figure 4, subtraction of the thus obtained spectrum of the sample annealed at 200 K (spectrum b) from that of the sample annealed at 160 K (spectrum a) gives the septet (spectrum c) characteristic of the $G(C8)H^{\bullet}$ radical,[19,20] as supported by the line shape simulation with the use of spectral parameters reported by Wang and Sevilla.[20] This radical can be formed by $H^{\bullet}$ atom addition to the double bond of nucleobase at the C8 position, or by protonation of the electron scavenging product (vide infra).

**$G^{-\bullet}$ Radical Anion.** In irradiated glassy systems containing DNA constituents, the radical anions of nucleobases are formed at 77 K and below due to scavenging of electrons ejected from water molecules.[2,13,21−23] The guanine radical anion, $G^{-\bullet}$, has been identified in ESR spectra as a singlet with the peak-to-peak width of ∼8−9 G.[21,24,25]

A signal attributable to $G^{-\bullet}$ was extracted by the procedure illustrated in Figure 5. First, we have removed from the initial spectrum (top spectrum in Figure 2) the normalized benchmark signal of $OH^{\bullet}$ radicals (cf., Figure 1). From the resulting pattern (spectrum a in Figure 5), we have subtracted the experimental spectrum of the sample annealed at 120 K (spectrum b; $OH^{\bullet}$ no longer present). The obtained difference spectrum (c) consists of a singlet with the peak-to-peak width of 8.3 G and some contribution of the $G(C8)H^{\bullet}$ signal in reverse-phase. The latter is due to the fact that annealing at 120 K leads to protonation of some radical anions at C8 position with formation of additional $G(C8)H^{\bullet}$ radicals; an increase of the amplitude of the high-field line of $G(C8)H^{\bullet}$ (∼3406 G, Figure 2) is evident in the total spectra.

Spectrum d in Figure 5, obtained by adding an appropriate amount of the $G(C8)H^{\bullet}$ septet to (c) (to get rid of the reverse-phase external wings), is in agreement with the simulated signal of the $G^{-\bullet}$ radical anion.[26,27] In support of our assignment, a similar singlet can be obtained as a difference between spectra A and B of Figure 3, from which $G(C8)H^{\bullet}$ signal has been first removed. It is well-known that radical anions are prone to photobleaching. We have to mention here that the $G^{-\bullet}$ signal cannot be completely removed on prolonged exposure to light because the HGW, unlike aqueous glasses of concentrated electrolytes, is not fully transparent (cf., Experimental Section).

**$dR(-H)^{\bullet}$ Radical.** Analysis of the spectra of dGMP-derived radicals, A or B in Figure 3, indicates that one more spectral component must be included. Figure 6 presents spectrum A after subtraction of the $G(C8)H^{\bullet}$ contribution according to the intensity of external lines. A doublet spectrum can be obtained as a result of its "titration" with the $G^{-\bullet}$ singlet.

A quite similar spectrum was observed by Sevilla et al. in γ-irradiated hydrated DNA samples after annealing at 235 K, and it was assigned to $G(C8)OH^{\bullet}$ radicals formed via hydration of the radical cation $G^{+\bullet}$, the product of direct radiation effect.[28] In our system, however, this direct effect is negligible[29] and $G^{+\bullet}$ is not produced.[30] Besides, the doublet is detected at 77 K, so we would rather have to consider another mechanism of $G(C8)OH^{\bullet}$ formation, viz., $OH^{\bullet}$ addition to the double bond of guanine base. Yet there is no evidence of such reaction at higher temperatures when $OH^{\bullet}$ radicals are released from their traps (vide infra).

It seems more plausible to assign spectrum c in Figure 6 to radicals formed by hydrogen atom abstraction from the deoxyribose moiety of dGMP, $dR(-H)^{\bullet}$. Such species, generated by different types of radiation, were identified in single crystal ENDOR studies[26,31] as well as in ESR studies of hydrated DNA and aqueous systems containing guanine nucleosides and nucleotides.[27,32−36] Recently, Sevilla et al. demonstrated that sugar radicals can be also produced by photoexcitation of $G^{+\bullet}$.[37−39] Considering the reported spectral parameters, we infer that our doublet spectrum can be assigned to the radical centered at C5′, cf., simulated signal in Figure 6.

**Reconstruction of the Spectra and Yields of Radicals Trapped at 77 K.** Using the benchmark signals of $OH^{\bullet}$, $HO_2^{\bullet}$ (cf., Figure 1), $G(C8)H^{\bullet}$ (c in Figure 4), $G^{-\bullet}$ (d in Figure 5), and $dR(-H)^{\bullet}$ (c in Figure 6), we have reconstructed the spectra recorded at the microwave power 0.02 mW for the initial sample, photobleached sample, and that annealed at 120 K (with no photobleaching); the results are presented in Figure 7A−C,

**SCHEME 1: Mechanism of Radical Formation at the L-type Defect Site in the Presence and in the Absence of dGMP**

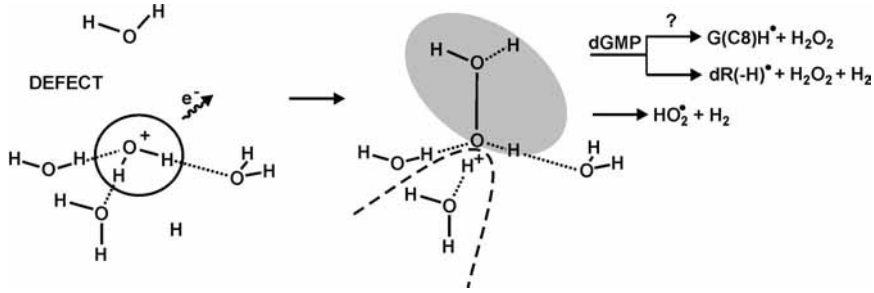


respectively. Table 1 summarizes relative contributions of radiation-produced radicals.

As seen from Table 1, contribution of oxygen radicals in the initial sample is 60%, and among organic radicals $G^{-\bullet}$ and dR(−H)• are almost equally abundant. An important finding is that the $[HO_2^\bullet]/[OH^\bullet]$ ratio is significantly lower in the presence of dGMP than in neat HGW (∼0.6 as compared to 1). According to our earlier suggestion,[9,13] this indicates that some neutral dGMP radicals are formed at the expense of $HO_2$ radicals at L-type defect sites as illustrated by Scheme 1.

We notice that for the initial spectrum the difference between OH• and $HO_2^\bullet$ fractions is equal to the relative contribution of dR(−H)•. This result suggests that the amount of G(C8)H• formed by the mechanism shown in Scheme 1 is negligible; apparently protonation of $G^{-\bullet}$ is a predominant reaction path of the H-adduct formation in our system at 77 K.

The reconstruction data for the photobleached sample confirm our qualitative observations described above: due to the light effect, the fraction of $G^{-\bullet}$ significantly decreases, and that of G(C8)H• increases. In addition, there is a pronounced decay of sugar radicals. These findings may be explained in terms of the reaction of electrons, ejected from $G^{-\bullet}$, with protons, leading to hot H atoms, which may add to dGMP molecule (growth of G(C8)H•) or combine with dR(−H)• (loss of the radical). Some of these electrons may also react with OH• radicals, although the observed decrease of OH• fraction (cf., Table 1) is close to the uncertainty of our determinations.

**Thermal Stability and Transformations of Radicals.** Figure 8 (upper panel) shows changes of the total concentration of radicals as a function of annealing temperature for the sample containing dGMP, as compared to neat HGW. As already mentioned, the least stable species is the OH• radical, which is no longer observed in our samples annealed at 120 K. Previous studies of the neat matrix[7] showed that it decays effectively around 100 K, well below the glass transition temperature of HGW ($T_g \approx 136$ K[15,40,41]), while $HO_2^\bullet$ radicals become mobile in the vicinity of $T_g$ and decay completely at a temperature close to that of cubic ice crystallization, $T_c \approx 160$ K.[42,43] In the presence of dGMP, the amounts of radicals lost in the temperature regions 77−120 and 120−150 K are not lower than the initial yields of OH• and $HO_2^\bullet$, respectively. This result indicates that thermally released oxygen radicals from the matrix do not react with the solute to produce another paramagnetic species. The lack of OH• reactivity is further supported by the fact that the spectrum of the sample annealed at 120 K can be well reconstructed using the same components as for the initial spectrum, and there is no increase (within uncertainty) in the contribution of sugar radicals, a possible product of OH• reaction, cf., Figure 7 and Table 1.

Recombination of $HO_2^\bullet$ leads to formation of molecular oxygen, which can react with dGMP-derived radicals to give peroxyl radicals, $RO_2^\bullet$, evident in the spectrum of the sample annealed at 210 K. Using this spectrum (recorded at 20 dB) as a benchmark signal of $RO_2^\bullet$, we were unable, however, to reconstruct with an acceptable quality the spectra of samples annealed at and above 150 K. Relative changes of $RO_2^\bullet$ concentration, presented in Figure 8, were estimated from intensities of the $g_{||} = 2.0356$ line in the respective spectra after subtraction of the G(C8)H• signal.

The yields of G(C8)H• in samples annealed at higher temperatures could be determined by scaling amplitudes of its high-field line (cf., Figure 2) for the integrated intensity of the respective benchmark. As noticed above, the growth of this radical in the range from 77 to 150 K is due to protonation of $G^{-\bullet}$ (some growth was also observed in the photobleached sample). It is seen from Figure 8 that the decay of G(C8)H• is accompanied by a growth of $RO_2^\bullet$, and total concentration of radicals in the temperature range 160−210 K remains fairly constant. This suggests that the H-adducts are precursors of $RO_2^\bullet$ radicals whose likely structure is presented in Chart 2; we assume $O_2$ addition to C4 (spin density 0.13, cf., ref 44) rather than to nitrogen, taking into account that carbon centers are more readily oxidized than are heteroatom centers.[45] It is important to add here that we do not exclude a possibility of $O_2$ addition to dR(−H)• radicals.

After decay of peroxyl radicals, a wide singlet remains in the spectrum, cf., Figure 2; its origin is yet obscure. It is rather not due to a primary species formed at 77 K, because the initial spectrum can be well reproduced without this signal. Such a singlet might be considered as a superposition of some $G^{-\bullet}$ and dR(−H)•, but it seems doubtful that the anion radicals survive matrix transformation to ice *Ih*, which has a maximum at ∼230 K.[43] Another possible explanation is that the signal corresponds to the electron-gain product protonated at O6 position. Formation of this species was reported for liquid solutions[46] and for single crystals of hydrated guanine hydrochloride;[31,47,48] in the latter system, it was observable up to about 250 K.

The ultimate radical decay can be related to transition of cubic ice into hexagonal ice.[43]

**Extent of Indirect Radiation Effects in the HGW Matrix.** The main indirect radiation effect in the examined system is electron scavenging by the solute. Our results indicate that despite a homogeneous solute distribution in the HGW matrix, OH• radicals do not react with dGMP, neither at 77 K nor on their detrapping at higher temperatures. This is a rather unexpected observation, which contrasts those reported for liquid solutions of DNA constituents[46,49] where OH• undergoes addition to the double bond of the base or abstracts H atom from the sugar moiety and, in the case of thymine derivatives, from the methyl group. The products of such reactions were also reported for the irradiated 7 mol/dm$^3$ $BeF_2$ glass heated to about 140 K.[22,27]

The results for HGW may be rationalized by assuming that for the low solute concentrations used in our study H-bonding

between water molecules extends over relatively large distances, without interference by a solute, so that the $OH^{\bullet}$ radicals recombine with each other via the mechanism of hydrogen transfer within the H-bonded structure,[16] before they encounter a solute molecule. One may expect that in aqueous electrolyte glasses, due to high concentration of ions, the tetrahedral arrangement of water molecules is considerably distorted.[50] This structural difference may be also the reason why in HGW, unlike in ionic glasses, trapped electrons are not observed even at 4 K.[51]

The second product of HGW radiolysis, $HO_2^{\bullet}$ radical, may be deemed an apparent reactive species. It is formed due to ionization of water molecules at the L-type defect sites, simultaneously with a hydrogen molecule and $H_3O^+$. In the presence of a solute, one of the hydrogen atoms involved in this concerted process may undergo addition to the double bond or H-abstraction reaction. In the case of dGMP, the latter reaction seems to occur only, leading to formation of $dR(-H)^{\bullet}$, and $H_2O_2$ molecule instead of the $HO_2^{\bullet}$ radical; cf., Scheme 1. Hence, HGW appears a good matrix to stabilize the products of H atom reactions with the solute under neutral pH conditions; in view of the proposed mechanism, it seems advisable to call these reactions water-mediated or pseudoindirect effects.

## Conclusions

In the $\gamma$-irradiated HGW matrix containing dGMP, three paramagnetic species are trapped at 77 K, along with $OH^{\bullet}$ and $HO_2^{\bullet}$ radicals from water: $G^{-\bullet}$ radical anion, H-adduct $G(C8)H^{\bullet}$, and the product of H abstraction from the sugar moiety (most probably at the C5′ site). Sugar radicals are created in competition with $HO_2^{\bullet}$ radicals at L-type defect sites of the H-bonded HGW matrix.

In the temperature range 120−150 K, additional $G(C8)H^{\bullet}$ radicals are formed by the C8-protonation of $G^{-\bullet}$. At and above 150 K (the point close to the temperature of crystallization to cubic ice), $G(C8)H^{\bullet}$ radicals are transformed to peroxyl radicals via reaction with the molecular oxygen produced upon $HO_2^{\bullet}$ recombination. A wide ESR singlet survives up to 250 K, where cubic ice is transformed into hexagonal ice, but its assignment is ambiguous.

The relevant conclusion of this study is that HGW is a good matrix to follow water-mediated radiation effects due to H atom reactions with the solute (under neutral pH-conditions), in addition to indirect effects due to electron scavenging. It is also inferred that the H-bonded structure in HGW is much more effective in recombining $OH^{\bullet}$ radicals than that of aqueous glasses consisting of highly concentrated electrolytes; no $OH^{\bullet}$ reactivity toward dGMP was observed either at 77 K or at higher temperatures.

**Acknowledgment.** This work has been supported by the Ministry of Science and Information Society Technologies in Poland (grants 3 T09A 057 26, 2004−2006, and SPB/COST 103/2005−2007). J.S. thanks the COST P9 Action for the STSM grant, which allowed her to discuss the results with the coauthors in Innsbruck and to prepare the samples for further studies. We also thank Micheal D. Sevilla, David Backer, and Amitava Adhikary (Oakland University, Rochester, MI) for helpful discussions on our results, Malgorzata Uglik (undergraduate student) for participation in some experiments, and Jan Pietek for writing the program for reconstruction of ESR spectra.

## References and Notes

(1) (a) Reviewed by: Niemann, E.-G. In *Biophysik*; Hoppe, W., Lohman, W., Markl, W., Ziegler, H., Eds.; Springer-Verlag: Berlin,1982; pp 300−312. (b) Ferradini, C. J. *J. Chim. Phys.* **1991**, *88*, 873. (c) von Sonntag, C. *Int. J. Radiat. Biol.* **1994**, *64*, 19.

(2) Sevilla, M. D.; Becker, D. Specialist Periodical Reports. *R. Soc. Chem.* **1994**, *14*, 129–165.

(3) Hutterman, J. In *Radical Ionic Systems*; Lund, A., Shiotani, M., Eds.; Kluwer Academic: Norwell, MA, 1991; pp 435−462.

(4) Franks, F. *Biophysics and Biochemistry at Low Temperatures*; Cambridge University Press: Cambridge, 1985; Chapter 3, pp 37−61.

(5) Szajdzinska-Pietek, E.; Bednarek, J.; Plonka, A.; Hallbrucker, A.; Mayer, E. *Res. Chem. Intermed.* **2001**, *27*, 937.

(6) Wang, W.; Razskazovskii, Y.; Sevilla, M. D. *Int. J. Radiat. Biol.* **1997**, *71*, 387.

(7) Bednarek, J.; Plonka, A.; Hallbrucker, A.; Mayer, E.; Symons, M. C. R. *J. Am. Chem. Soc.* **1996**, *118*, 9387.

(8) Bednarek, J.; Plonka, A.; Hallbrucker, A.; Mayer, E. *J. Phys. Chem. A* **1998**, *102*, 9091.

(9) Bednarek, J.; Plonka, A.; Hallbrucker, A.; Mayer, E. *J. Phys. Chem. B* **1999**, *103*, 6824.

(10) Plonka, A.; Szajdzinska-Pietek, E.; Bednarek, J.; Hallbrucker, A.; Mayer, E. *Phys. Chem. Chem. Phys.* **2000**, *2*, 1587, and references therein.

(11) Mayer, E. *J. Appl. Phys.* **1985**, *58*, 663.

(12) Devlin, J. P. *Int. Rev. Phys. Chem.* **1990**, *9*, 29.

(13) Staluszka, J.; Plonka, A.; Szajdzinska-Pietek, E.; Kohl, I.; Hallbrucker, A.; Mayer, E. *Radiat. Phys. Chem.* **2003**, *67*, 247.

(14) Bowron, D. T.; Finney, J. L.; Hallbrucker, A.; Kohl, I.; Loerting, T.; Mayer, E.; Soper, A. K. *J. Chem. Phys.* **2006**, *125*, 194502.

(15) Kohl, I.; Bachmann, L.; Hallbrucker, A.; Mayer, E.; Loerting, Th. *Phys. Chem. Chem. Phys.* **2005**, *7*, 3210.

(16) Plonka, A.; Staluszka, J.; Szajdzinska-Pietek, E.; Kohl, I.; Hallbrucker, A.; Mayer, E. *Res. Chem. Intermed.* **2003**, *29*, 63.

(17) Sevilla, M. D.; Becker, D.; Yan, M.; Summerfield, S. R. *J. Phys. Chem.* **1991**, *95*, 3409.

(18) Bednarek, J.; Plonka, A.; Hallbrucker, A.; Mayer, E. *Radiat. Phys. Chem.* **1998**, *53*, 635.

(19) Wang, W.; Sevilla, M. D. *Int. J. Radiat. Biol.* **1994**, *66*, 683.

(20) Wang, W.; Sevilla, M. D. *Radiat. Res.* **1994**, *138*, 9.

(21) Bernhard, W. A. *J. Phys. Chem.* **1989**, *93*, 2187.

(22) Ohlmann, J.; Huttermann, J. *Int. J. Radiat. Biol.* **1993**, *63*, 427.

(23) Barnes, J. P.; Bernhard, W. A. *J. Phys. Chem.* **1995**, *99*, 11248.

(24) Yan, M.; Becker, D.; Summerfield, S.; Renke, P.; Sevilla, M. D. *J. Phys. Chem.* **1992**, *96*, 1983.

(25) Sevilla, M. D.; Failor, R.; Clark, C.; Holroyd, R. A.; Pettei, M. *J. Phys. Chem.* **1976**, *80*, 353.

(26) Hole, E. O.; Nelson, W. H.; Sagstuen, E.; Close, D. M. *Radiat. Res.* **1992**, *129*, 119.

(27) Przybytniak, G. Institute of Nuclear Chemistry and Technology Reports; Series A, No 3/2004; Warsaw, 2004 (in Polish).

(28) Shukla, L. I.; Adhikary, A.; Pazdro, R.; Backer, D.; Sevilla, M. D. *Nucleic Acids Res.* **2004**, *32*, 6565.

(29) Our experiments for HGW systems containing other nucleotides (dTMP, dCMP) show that increasing the solute concentration from 5 to 50 mmol $dm^{-3}$ does not lead to any new ESR component, and relative contributions of individual species to the total spectrum of organic radicals are not affected within uncertainty $<10\%$ (unpublished results). This proves that the mechanism of radiolysis remains the same in the examined concentration range.

(30) The spectrum of the radical cation represents a relatively broad unresolved singlet with the apparent *g*-value (experimental center of the spectrum) higher than that of $G^{-\bullet}$ (cf., ref 17) and that of the wide singlet observed in our system annealed at 250 K (cf., Figure 2).

(31) Strand, P.; Sagstuen, E.; Lehner, T.; Huttermann, J. *Int. J. Radiat. Biol.* **1987**, *51*, 303.

(32) Weiland, B.; Huttermann, J. *Int. J. Radiat. Biol.* **1998**, *74*, 341.

(33) Weiland, B.; Huttermann, J. *Int. J. Radiat. Biol.* **1999**, *75*, 1169.

(34) Becker, D.; Bryant-Friedrich, A.; Trzasko, C. A.; Sevilla, M. D. *Radiat. Res.* **2003**, *160*, 174.

(35) Shukla, L. I.; Pazdro, R.; Becker, D.; Sevilla, M. D. *Radiat. Res.* **2005**, *163*, 591.

(36) Przybytniak, G.; Huttermann, J.; Ambroz, H.; Weiland, B. *Nukleonika* **1997**, *42*, 323.

(37) Shukla, L. I.; Pazdro, R.; Huang, J.; DeVreugd, C.; Becker, D.; Sevilla, M. D. *Radiat. Res.* **2004**, *161*, 582.

(38) Adhikary, A.; Malkhasian, A. Y. S.; Collins, S.; Koppen, J.; Becker, D.; Sevilla, M. D. *Nucleic Acids Res.* **2005**, *33*, 5553.

(39) Adhikary, A.; Collins, S.; Khanduri, D.; Sevilla, M. D. *J. Phys. Chem. B* **2007**, *111*, 7415.

(40) Johari, G. P.; Hallbrucker, A.; Mayer, E. *Nature* **1987**, *435*, E1.

(41) Kohl, I.; Bachmann, L.; Mayer, E.; Hallbrucker, A.; Loerting, Th. *Nature* **2005**, *435*, E1.

(42) Hage, W.; Hallbrucker, A.; Mayer, E. *J. Chem. Phys.* **1994**, *100*, 2743.

(43) Kohl, I.; Mayer, E.; Hallbrucker, A. *Phys. Chem. Chem. Phys.* **2000**, *2*, 1579.

(44) Wetmore, D. S.; Boyd, R. J.; Eriksson, L. A. *J. Phys. Chem. B* **1999**, *102*, 9332.
(45) von Sonntag, C.; Schuchmann, H.-P. In *Peroxyl Radicals*; Alfassi, Z. B., Ed.; J. Wiley & Sons Ltd.: New York, 1997; Chapter 8.
(46) von Sonntag, C.; Schuchmann, H.-P. In *Radiation Chemistry. Present Status and Future Trends*; Janah, C. D., Rao, B. S. M., Eds.; Elsevier: New York, 2001; pp 513−551.
(47) Close, D. M.; Nelson, W. H.; Sagstuen, E. *Radiat. Res.* **1987**, *112*, 283.
(48) Nelson, W. H.; Hole, E. O.; Sagstuen, E.; Close, D. M. *Int. J. Radiat. Biol.* **1988**, *54*, 963.
(49) Steenken, S. *Chem. Rev.* **1989**, *89*, 503.
(50) Suzuki, Y. *Chem. Phys. Lett.* **2001**, *335*, 375, and references therein.
(51) Bednarek, J.; Plonka, A.; Hallbrucker, A.; Mayer, E. *Radiat. Phys. Chem.* **1999**, *55*, 477.

JP8037544